Journal of CO2 Utilization 80 (2024) 102698

Contents lists available at ScienceDirect

Journal of CO2 Utilization

journal homepage: www.elsevier.com/locate/jcou

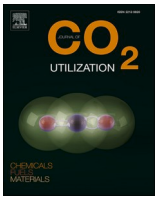

The influence of α,ω-diols and SiO_2 particles on CO_2 absorption and NH_3 escaping during carbon dioxide capture in ammonia solutions

Temesgen Abeto Amibo [a,b,1], Donata Konopacka-Łyskawa [b,*,2]

[a] Gdańsk University of Technology, Faculty of Chemistry, Department of Process Engineering and Chemical Technology, Narutowicza 11/12, 80-233 Gdańsk, Poland
[b] Gdańsk University of Technology, School of Chemical Engineering, Jimma Institute of Technology, Jimma University, P.O. Box-378, Jimma, Ethiopia

ARTICLE INFO

Keywords:
Carbon capture
Ammonia escape
α,ω-diols
Silica particles
Mass transfer

ABSTRACT

Ammonia solutions are widely used solvents for CO_2 capture. However, a significant disadvantage of these solvents is secondary pollution of the purified gas stream by desorbed ammonia. In this work, α,ω-diols, and colloidal silica have been proposed to reduce this undesired effect. Ammonia solutions with the addition of ethylene glycol (EG), 1,3-propanediol (PRD), 1,4-butanediol (BUD), 1,5-pentanediol (PED), or 1,6-hexanediol (HED) and ammonia solution with the addition of diol and colloidal SiO_2 were tested. The concentration of CO_2 and NH_3 in the exhaust gas was continuously measured during the experiments. Based on the recorded measurements, the number of moles of CO_2 absorbed and the number of moles of NH_3 lost were calculated. Mass transfer coefficients for CO_2 absorption and NH_3 desorption were also determined. The studies showed that CO_2 absorption occurred faster in ammonia solutions with EG, PRD, BUD, and HED, and the CO_2 loading was higher than in pure NH_3 solution. The most effective additive improving CO_2 absorption was BUD, followed by HED. SiO_2 particles improved slightly the absorption efficiency in most of the tested diol solutions. All diols used inhibited the escape of ammonia, with PED having the most effective effect. However, adding silica particles effectively inhibited ammonia escape in all tested systems.

1. Introduction

The world has become increasingly concerned due to the rising levels of CO_2 in the atmosphere. The high concentration of CO_2 in the atmosphere contributes to global warming and it also leads to the melting of polar ice caps, exacerbates food shortages and insecurity, and renders our planet increasingly inhospitable for both humans and other living organisms [1,2]. Despite the efforts of researchers actively engaged in ongoing studies and implemented technologies, the results of these actions have not been as effective in mitigating CO_2 concentrations as anticipated. The causes behind escalating CO_2 levels can be categorized into two main sources: human activities and natural processes [3,4]. The primary contributors to CO_2 emissions include natural phenomena like the weathering of carbonated rocks, volcanic eruptions, and biological respiration. Nevertheless, these natural processes do not significantly elevate CO_2 concentrations compared to the impact of human activities. Notably, numerous studies have pointed to a 20% increase in CO_2 emissions over 42 years, primarily attributed to fossil fuel combustion, making it the predominant human-induced source of CO_2 increases in the atmosphere [5].

In ongoing efforts to reduce carbon footprint and mitigate the impacts of climate change, various methods were explored. Some of these, like photosynthesis and the natural occurrence of acid rain, are inherent processes in our environment. On the other hand, there are developed greenhouse gas reduction methods to minimize their concentration in the atmosphere. Among these methods, a large group are the processes of carbon capture, utilization and storage [6]. All proposed solutions require CO_2 capture. There are three options for CO_2 capture: post-conversion, pre-conversion and oxy-fuel combustion [7]. During pre-conversion capture, absorption in chemical and physical solvents as well as adsorption by porous organic frameworks is most often used, while post-conversion capture is carried out using processes such as physical and chemical absorption, adsorption, membrane separation, cryogenic separation, or separation with using microbial/algal systems [7,8]. However, the principle of oxy-fuel combustion involves the use of pure oxygen in processes, thanks to which an almost pure stream of CO_2

* Corresponding author.
E-mail addresses: temesgen.amibo@pg.edu.pl (T.A. Amibo), donata.konopacka-lyskawa@pg.edu.pl (D. Konopacka-Łyskawa).
[1] ORCID 0000-0003-2574-3129
[2] ORCID 0000-0002-2924-7360

https://doi.org/10.1016/j.jcou.2024.102698
Received 10 November 2023; Received in revised form 12 January 2024; Accepted 29 January 2024
Available online 2 February 2024

is obtained after the process [7]. Ideas for utilization and storing CO_2 are very diverse and include solutions such as turning carbon dioxide into beverages, injecting it deep within the Earth's crust and storage in saline formation, CO_2 enhancement oil recovery, and the use of CO_2 as a reagent for the production of various chemical compounds [9]. Examples of important chemicals produced from CO_2 are urea, methanol, cyclic and linear carbonates, carboxylic acids, esters, lactones, concrete, polymers, and fine chemicals [10,11]. Additionally, technologies are being developed to manage carbon dioxides and calcium-rich wastes, e.g., post-distillation liquid from the Solvay process, metallurgical slag from steel production, cement industry waste, gypsum waste, ash from paper sludge, and oil shale ash to the production of calcium carbonate [12]. All these attempts contribute to reducing CO_2 levels and offer prospects for sustainable solutions in the fight against climate change [13].

Among the proposed carbon dioxide capture methods, absorption is one of the most established technologies [14]. This process can be carried out using physical solvents such as dimethyl ether of polyethylene glycol utilized in Selexol process, methanol used in Rectisol method, and fluorinated solvents, in which only the dissolution of the absorbed component occurs in the entire volume of the solution, or as chemical absorption when a reaction occurs between the absorbed compound and the component(s) of the liquid phase. Solvents used in chemical absorption are solutions of amines (e.g. monoethanolamine MEA, diethanolamine DEA, methyldiethanolamine MDEA), ammonia, potassium carbonate, and ionic liquids.

Currently, most CO_2 capture technologies are based on absorption in amine solutions. However, ammonia has recently been indicated as a promising solvent for these applications. The selection of this absorbent is based on its cost-effectiveness, stability, resistance to degradation in the presence of oxygen and sulfur oxide, reduced energy consumption, and exceptional carbon capture efficiency. However, the main challenge with this solvent is the high volatility of ammonia and the tendency to escape during gas flow. This results in the loss of a critical component of the absorbent and contributes to secondary pollution, necessitating additional operations to recover ammonia from the gas stream after absorption [15].

Hence, miscellaneous strategies are used to reduce the presence of ammonia in the separated gas. The foremost methods of inhibiting ammonia escape include scrubbing techniques such as water washing and acid washing, optimization of absorber operation minimizing ammonia desorption, and utilization of various organic and inorganic additives, causing ammonia retention in the solvent [14]. The absorption of ammonia in water or acid is a very effective method of removing this component from gases, but it requires additional installations for gas purification and solvent regeneration. Process optimization includes fine-tuning parameters such as ammonia concentrations in the solution, managing pH levels, adjusting reaction temperatures, and monitoring CO_2 loading and partial pressure [14,16]. Another strategy being developed is the utilization of inhibitors of ammonia escape from the absorbent. Inorganic additives are metal ions that form complexes with ammonia, e.g., Cu^{2+}, Ni^{2+}, Zn^{2+}, Co^{2+} [17–19]. On the other hand, organic compounds that slow down the escape of ammonia are primarily compounds containing hydroxyl groups [20,21]. Recently, research has been carried out on new biphasic absorbents for CO_2 capture [22–24]. Their unique operation is based on two immiscible liquid phases formation after CO_2 absorption, differing significantly in CO_2 concentration. These solvents can be obtained, among others, by mixing a solution of amine and alcohol or poly(ethylene glycol) dimethyl ether. It has been shown that compounds containing hydroxyl groups can increase the overall mass transfer coefficient during absorption and benefit solvent regeneration [24]. A new approach to improving CO_2 absorption is the application of nanofluids, i.e., liquids containing nanoparticles [25]. Research shows that even a small concentration of nanoparticles in the absorbent can significantly increase the rate of CO_2 absorption [26]. Moreover, recently published studies conducted using an ammonia solution containing colloidal SiO_2 particles also confirmed the positive effect of this type of particle on the absorption process [27]. Fine SiO_2 particles at a concentration in the range of 0.01%− 0.15% considerably reduced the escape of ammonia.

In this research, selected diols and colloidal silica were employed to increase the CO_2 absorption rate and to prevent the escape of ammonia during carbon capture in ammonia solutions. The following α,ω-diol homologs: 1,2-ethane diol (ethylene glycol, EG), 1,3-propanediol (PRD), 1,4-butanediol (BUD), 1,5-propanediol (PRD), and 1,6-hexanediol (HED) were used as organic additives. Previous research has consistently indicated that organic additives with a higher number of hydroxyl groups exhibit superior inhibition of ammonia escape compared to those with fewer hydroxyl groups [20]. In addition, molecules in which the hydroxyl groups are separated from each other have a beneficial impact during the absorption of CO_2 in ammonia solutions. The novelty of this work is showing the influence of diols with different carbon chain lengths on the carbon dioxide absorption rate. Moreover, the effect of combined additives, i.e., organic compound and fine particles, on the rate of carbon dioxide absorption in ammonia solutions and the reduction of ammonia escape has not been previously tested. Therefore, in these studies, we assumed that the presence of diols and fine solid particles could have a synergistic effect on CO_2 capture in NH_3 solutions.

2. Materials and methods

2.1. Reagents

Absorbent used in these experiments were prepared from water obtained by reverse osmosis and 25% ammonia solution (POCH, Poland). Carbon dioxide gas was purchased from Linde Gas, Poland. The following α,ω-diols were added to absorbent solutions: 1,2-ethane diol (99.0%, Chempur, Poland), 1,3-propane diol (99.0%, Thermo-Scientific, Germany), 1,4-butane diol (99.0%, Acros-Organics, Taiwan), 1,5-pentane diol (98.0%, Thermo-Scientific, Spain), and 1,6-hexane diol (97.0%, Thermo-Scientific, Germany). These substances were referred to as organic additives. Some experiments used Silica Aerosil® 200 (>99.8%, Evonik, Germany).

The methodology employed in this study centers around the liquid-gas reaction mechanism. Within the mini reactor, a liquid solution comprising ammonia (NH_3), additives, and nano-silica (SiO_2) is meticulously prepared in accordance with predetermined quantities to ensure uniformity. To achieve consistent dispersion of nanoparticles in the solution, nanosilica undergoes a 30-minute ultrasonic treatment. Subsequently, a gas mixture composed of carbon dioxide and air is introduced into the reactor. The theoretical reaction time, calculated based on the mole ratios of ammonia and carbon dioxide, serves as the time limit for complete reaction. Once the ammonia and carbon dioxide have undergone full reaction, the flue gas valve is sealed. These experiments are conducted under conditions of room temperature and atmospheric pressure.

2.2. Apparatus and methods

2.2.1. CO_2 absorption experiments

Carbon dioxide absorption measurements and inhibiting ammonia escape were carried out in the bubble reactor with a volume of 0.5 dm^3 . A sparger made with sintered glass for even gas dispersion throughout the solution was used in the reactor. The proper distribution of the gas in the ammonia solution was created by the deep and vertical insertion of a gas distributor into the solution. The flow rate of the gas mixture was set by mass controllers at 0.5 dm^3/min with the CO_2 volume fraction in air equal to 0.15. Gas components were mixed within an in-line mixer before being introduced into the reactor. The outlet gas with unabsorbed CO_2 and desorbed NH_3 was diluted in the mixing chamber with the fresh air to maintain concentrations below the predetermined operating limit of gas sensors. The diaphragm pump rotation speed controlled the

volume gas flow rate through the chamber. The CO_2 and NH_3 concentration in the diluted gas stream was analyzed by the infrared CO_2 sensor Gravity produced by DFRobot and the electrochemical NH_3 sensor from the SGX Sensortech An Amphenol Company, respectively. The sensors were placed in separate Teflon chambers to limit the adsorption of the analyzed compound and avoid its undesirable transformation. The signals from gas sensors were recorded using an analog-to-digital converter. The Arduino MEGA 2560 Rev3 control module was used to control automatically the custom-built system. The complete arrangement for the carbon dioxide absorption setup is presented in Fig. 1. Based on the calibration, the signals from the sensors were used to determine the concentration of ammonia and carbon dioxide in the outlet gas stream as a volume fraction.

Aqueous solutions of ammonia with NH_3 concentration of 1.5 mol/dm^3 were used as solvents for CO_2 absorption. The concentration of diols added to the solvent was 0.3 mol/dm^3, and the amount of added silica was 0.05 wt%. The amount of used SiO_2 was selected based on previously conducted tests, in which the best effect of slowing down the escape of ammonia was achieved for this concentration [27]. To obtain a stable dispersion during measurements, the initial suspension of SiO_2 particles in water was prepared and sonicated in an ultrasonic bath for 30 min. Then the right amount of commercial ammonia solution, organic additive and the rest of the water were added to obtain the assumed concentrations of ammonia in the tested solvent. The volume of the tested absorbent was 0.300 dm^3 in each experiment. CO_2 absorption in a tested solvent was carried out for 60 min pH of solutions were measured during CO_2 absorption.

2.2.2. Determination of physical properties

Density measurements of ammonia solutions with organic additives were made using a DMA 1001 density meter (Anton Paar). Before each series of measurements, calibration was performed using ultrapure water and air. The dynamic viscosity of the solutions was determined in a Brookfield LVDV-II + rotational viscometer equipped with an attachment for small-volume samples. The surface tension of the used solution was measured using the tensiometer Krüss K11 applying the Wilhelmy plate method [28]. Before surface tension measurement, calibration was performed in ultrapure water. Each measurement was repeated a minimum of three times.

3. Result and discussion

3.1. Physical properties of solvents

The basic physical properties of solvents significantly impact the mass transfer during both the absorption and desorption processes. Therefore, the solutions' density and viscosity were determined and the obtained values are in Table 1.

The measured density and viscosity of the used ammonia solution without and with dioles do not significantly vary. However, diol solutions differ in their surface activity. In the case of ethylene glycol, 1,3-propanediol and 1,4-butanediol, The increase in the number of carbon atoms in the diol molecule resulted in a slight decrease in the surface tension of the solutions. However, pentanediol and hexanediol reduced the surface tension of aqueous ammonia solutions from 69.6 to 51.8 and 56 mN/m, respectively. Similar surface properties of α,ω-diols were obtained for their aqueous solutions (without ammonia) [29,30], and the lowest surface tension characterized aqueous solutions containing PED [31].

3.2. Carbon dioxide absorption

The change in carbon dioxide concentration in the gas outlet stream over time is shown in Fig. 2 and Fig. 3. The recorded CO_2 concentration output curves in the gas stream can be divided into three ranges. The initial period is very short, lasts about 40 s, and is characterized by the absence of carbon dioxide in the exhaust gas. This is due to the fact that all introduced CO_2 has been retained in the ammonia solution. Additionally, the gas must flow through the entire measuring system

Table 1
Physical properties of the used solvents at room temperature (23 °C).

Solution	ρ, kg·m^3	μ, mPa·s	σ, mN·m^{-1}
Control	989.48	1.04	69.6
EG	991.86	1.05	68.2
PRD	990.87	1.05	67.6
BUD	990.02	1.08	65.6
PED	989.97	1.05	51.8
HED	989.13	1.07	56.0

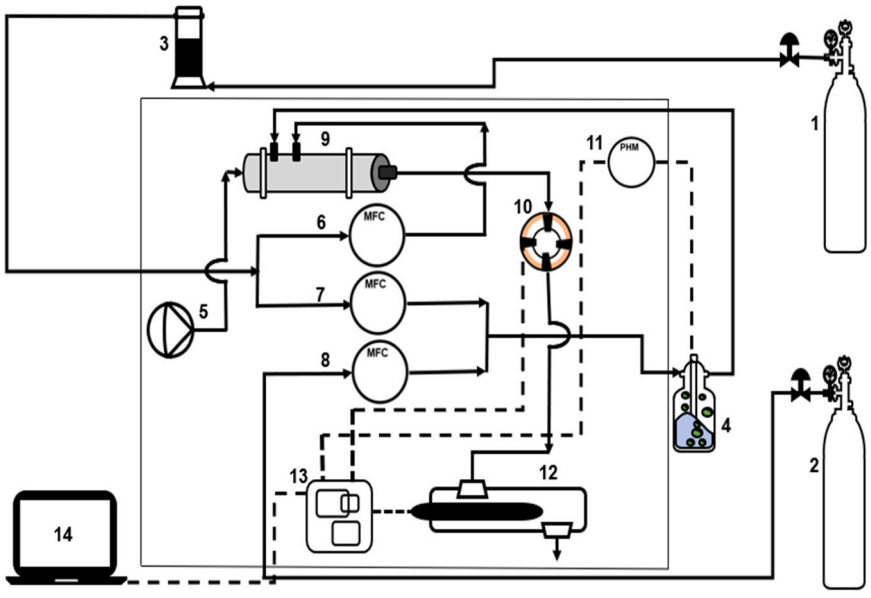

Fig. 1. Flow diagram of CO_2 absorption system: (1) the air cylinder equipped with a pressure gauge and valve, (2) the CO_2 cylinder equipped with pressure gauges and valves, (3) the adsorption column with NaOH, (4) the bubble reactor, (5) the pump, (6) and (7) the air mass flow controllers, (8) the CO_2 mass flow controller; (9) the gas mixer, (10) the ammonia sensor, (11) the pH sensor, (12) the carbon dioxide sensor, (13) the connector, and (14) the computer.

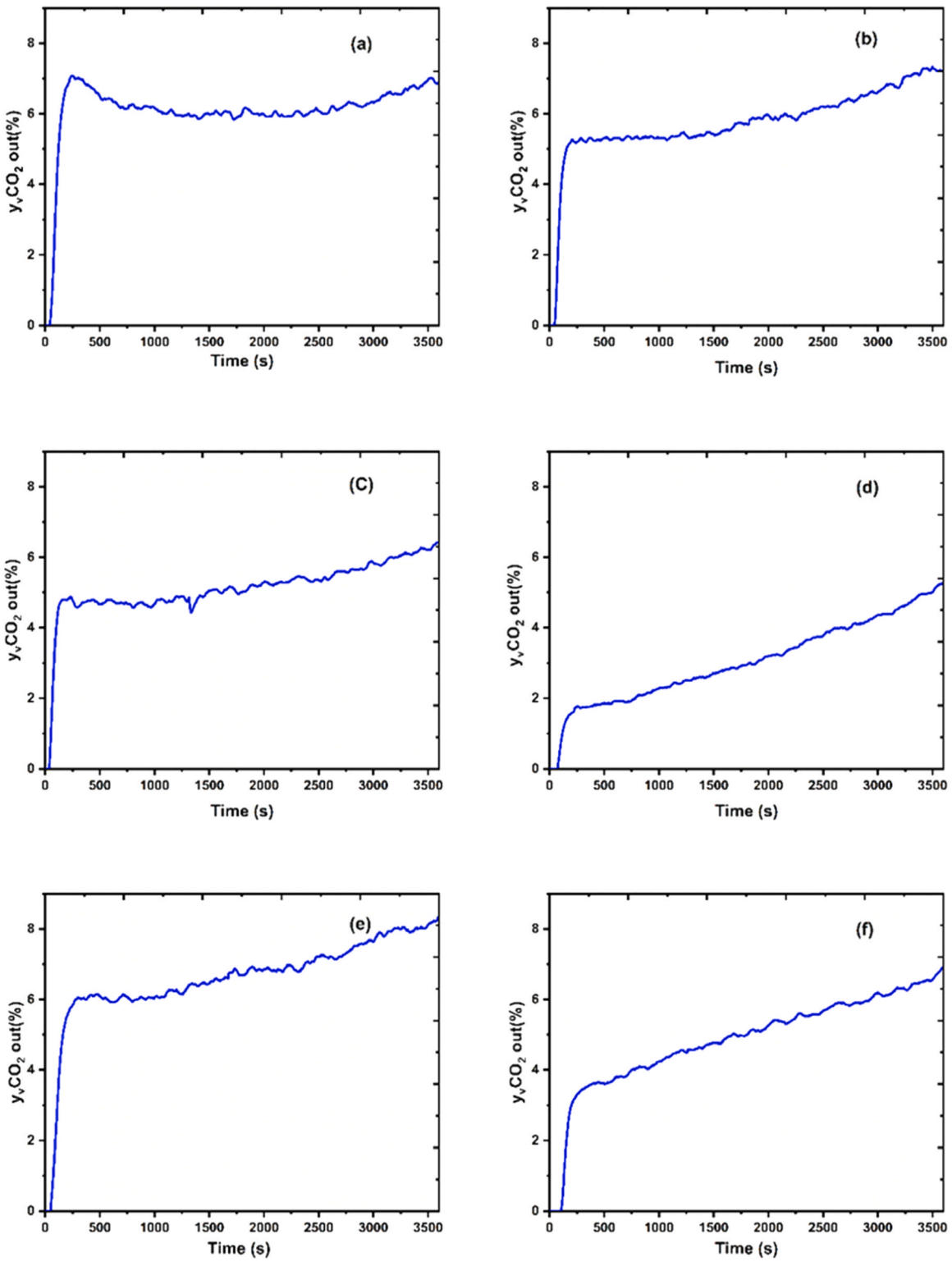

Fig. 2. The outlet mole fraction of CO_2 released from the solution containing organic additives: (a) control (without additives), (b) EG, (c) PRD, (d) BUD, (e) PED, (f) HED utilized.

immediately after starting the measurement. In the second period, a rapid increase in CO_2 concentration at the outlet from the absorber is visible. During this period, the differences in the output curves for the used organic additives are significant. The largest increase in CO_2 concentration at the beginning of this period was for the ammonia solution without additives and in the presence of 1,5-pentanediol. The CO_2 concentration increased the least after adding 1,4-butanediol and 1,6-butanediol. A similar course was observed for absorption in solvents with fine silica particles. In the next stage, the reactor operation is established, i.e. CO_2 is supplied to the absorber, part of the CO_2 is reacted, and the CO_2 not used in the reaction leaves the system in the flowing air stream. A practically constant absorption rate is observed for ammonia solution without additives and in the presence of ethylene glycol and propylene glycol. The longest absorption period

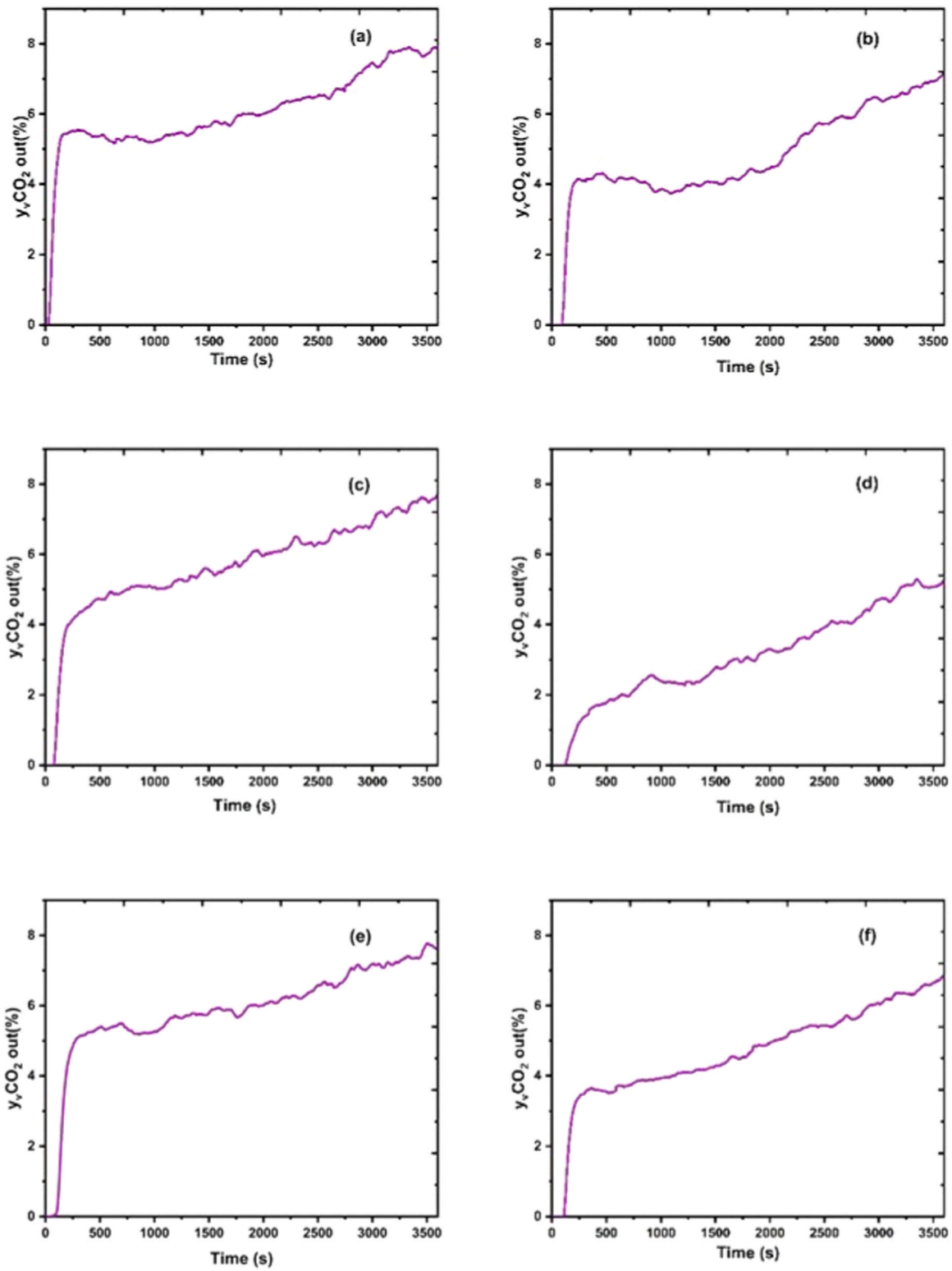

Fig. 3. The outlet mole fraction of CO_2 released from the solution containing organic additives and fine SiO_2 particles: (a) without diols; (b) EG; (c) PRD; (d) BUD; (e) PED; (f) HED.

characterized by a fixed CO_2 concentration in the exhaust gas was recorded for a pure ammonia solution (the end of stable period occurred after approximately 2200 s). In the case of measurements with silica particles, a constant absorption rate in the third range occurs for the ammonia solution without organic additives and with the addition of ethylene glycol. Then, at the final time of these experiments, the CO_2 concentration in the outlet gas slowly increased. In the tests made with 1,4-butanediol, 1,5-propanediol, and 1,6-hexanediol, the third absorption period was characterized by a slow increase in CO_2 concentration in exhaust gases throughout the investigated range of time.

Based on the molar stream of air introduced into the absorber and the concentration of CO_2 in the inlet and outlet streams at define time of

experiments, the efficiency of CO_2 capture in the tested absorbents was calculated as:

$$\alpha_{CO2} = \frac{n_{in,CO2} - n_{out,CO2}}{n_{in,CO2}} \bullet 100\% = \frac{\Delta n_{CO_2}}{n_{in,CO2}} \bullet 100\% \quad (1)$$

where: α_{CO_2} is the efficiency of carbon dioxide capture, $n_{in,CO2}$ is the number of moles of carbon dioxide introduced to the absorber, and $n_{out,CO2}$ is the number of moles of carbon dioxide flowing out with the exhaust gas from the absorber and Δn_{CO_2} is the number of moles of carbon dioxide remaining in the absorber.

The total molar flux of introduced CO_2 can be determined as:

$$Q_{in,CO2} = Q_{air} Y_{in,CO2} \quad (2)$$

where Q_{air} is the molar flux of air, $Y_{in,CO2}$ is the relative mole fraction of carbon dioxide in the inlet gas.

The total molar flux of absorbed CO_2 at given time can be calculated from:

$$Q_{CO2} = Q_{air}\left(Y_{in,CO2} - Y_{out,CO2}\right) \quad (3)$$

where $Y_{out,CO2}$ is the relative mole fraction of carbon dioxide in the outlet gas.

To determine the absorbed number of moles of CO_2 during the entire process time, the total CO_2 mole flux should be multiplied by the measuring time intervals and integrated.

The obtained results of CO_2 capture efficiency in the tested solvents are presented in Table 2.

The efficiency of CO_2 capture by ammonia solutions in the presence of the tested glycols was higher than in the NH_3 solution without additives. The only exception to this rule is the ammonia solution containing 1,5-pentanediol, in which the number of moles of absorbed CO_2 was 8% lower compared to the control absorbent. The most effective CO_2 absorbent was the NH_3 solution with the addition of 1,4-butanediol (71.7% CO_2 absorption efficiency) and with the addition of 1,6-hexanediol (66.7% CO_2 absorption efficiency). Comparing the obtained results of CO_2 capture in solutions without and with the addition of fine silica particles, it can be seen that the presence of SiO_2 in the used concentration 0.05 wt% does not significantly affect the efficiency of CO_2 removal from the gas stream for most of the organic additives tested. Only the CO_2 absorption was higher by approximately 6% in the ammonia solution with the addition of 1,5-pentanediol while these changes were not greater than 2% in the presence of other additives.

Considering the surface tension of the solvents used (Table 1), the impact of this parameter on the CO_2 absorption rate is unclear. The reduction of surface tension for EG, PRD, BUD, and HED is correlated with the increase in the absorption rate, while in the case of PED, the opposite trend is observed. Other studies also do not explain the influence of this physical property of the solution on the absorption process. On the one hand, reducing surface tension favors the formation of smaller gas bubbles in the bubble system, and then the interfacial surface area increases [32]. At the same time, adsorbed surfactant molecules can promote absorption and facilitate CO_2 transfer through the interface [33]. However, other results showed, that the adsorption of the surfactant at the gas-liquid interface can reduce or eliminate interfacial turbulence and place a surfactant barrier that makes it difficult to transfer the ingredient from the gas phase to the liquid phase, which reduces the absorption rate [34].

Table 2
Efficiency of CO_2 capture (α_{CO2}) and overall volumetric mass transfer coefficient of carbon dioxide absorption ($K_G a$) in ammonia solutions with the tested additives.

Solution	α_{CO2}, %		$K_G a \cdot 10^4$, mol·m^{-3}·s^{-1}·Pa^{-1}	
	without SiO_2	with SiO_2	without SiO_2	with SiO_2
Control	59.3	58.3	1.00	0.99
EG	62.2	63.8	1.09	1.14
PRD	64.2	64.2	1.17	1.09
BUD	71.7	73.5	1.34	1.47
PED	51.3	57.0	0.87	0.93
HED	66.7	67.4	1.22	1.28

Based on the obtained results of the CO_2 absorption rate in the tested solvents, the volumetric mass transfer coefficients were determined. For this purpose, the model proposed by Atzori *et al.* was adopted [35]. The CO_2 mass transfer from the gas phase to the liquid phase depends on the driving force of the CO_2 absorption, i.e., the difference in the partial pressures of this component in the gas phase and the liquid phase therefore the molar flow rate of CO_2 can be expressed as:

$$N_{CO2} = K_G\left(p_{G,CO2} - p_{L,CO2}\right) \quad (4)$$

where N_{CO2} is the molar flow rate of carbon dioxide, K_G is the overall mass transfer coefficient of carbon dioxide, $p_{G,CO2}$ and $p_{L,CO2}$ are partial pressures in the gas phase and liquid phase, respectively.

For the tested system, the average partial pressure of CO_2 in the gas phase was determined as the logarithmic mean value as proposed Ma *et al.* [16]:

$$p_{G,CO2} = P\frac{y_{in,CO2} - y_{out,CO2}}{\ln \frac{y_{in,CO2}}{y_{out,CO2}}} \quad (5)$$

where P is the total pressure in the system, $y_{in,CO2}$ and $y_{out,CO2}$ are mole fractions of CO_2 in the inlet and outlet gas stream, respectively.

The partial pressure of carbon dioxide in a liquid phase depends on the concentration of free CO_2 in the liquid $C_{L,CO2}$ and the Henry's constant H_L^{CO2}:

$$p_{L,CO2} = C_{L,CO2} H_L^{CO2} \quad (6)$$

To calculate the Henry's constant, the "NO_2 analogy" was applied:

$$H_L^{CO2} = H_L^{NO2}\left(\frac{H_w^{CO2}}{H_w^{NO2}}\right) \quad (7)$$

The dependence of Henry's constant on temperature (T) for NO_2 absorption in ammonia solution H_L^{NO2} is given by [36]:

$$H_L^{NO2} = \left(0.155 + 8.17 \bullet 10^{-3} \bullet C_L^{NH3}\right) \bullet 10^6 \exp\left(-\frac{0.00115}{T}\right) \quad (8)$$

where C_L^{NH3} is the concentration of free ammonia in the solution.

The Henry's constant for NO_2 absorption in water H_w^{NO2} was determined from the equation [37]:

$$H_w^{NO2} = \frac{10^5}{1.9}\exp\left[-1400\left(\frac{1}{T} - \frac{1}{298.15}\right)\right] \quad (9)$$

and the Henry's constant for CO_2 absorption in water was calculated as [37]:

$$H_w^{CO2} = \frac{10^4}{3.4}\exp\left[-2400\left(\frac{1}{T} - \frac{1}{298.15}\right)\right] \quad (10)$$

The concentration of free CO_2 was determined based on the number of moles of CO_2 absorbed in the tested solvent volume. The constants of reactions occurring in aqueous solutions in the presence of carbon dioxide and ammonia were taken in the calculations [35]:

$$H_2O \leftrightarrows OH^- + H^+ \quad (11)$$

$$CO_2 + H_2O \leftrightarrows HCO_3^- + H^+ \quad (12)$$

$$HCO_3^- \leftrightarrows CO_3^{2-} + H^+ \quad (13)$$

The concentration of free NH_3 was calculated using the dissociation constant of the reaction [35]:

$$NH_3 + H_2O \leftrightarrows NH_4^+ + OH^- \quad (14)$$

The molar flow rate of CO_2 N_{CO2} depends on the total molar flux Q_{CO2}determined from Eq. (3) and the gas-liquid interface area A:

$$N_{CO2} = \frac{Q_{CO2}}{A} = \frac{Q_{CO2}}{aV_L} \quad (15)$$

where a is a specific surface area (in the unit solution volume), and V_L is the volume of solution used in the experiment.

By combining relationships (3) – (15), the volumetric mass transfer coefficient for CO_2 absorption K_Ga was determined. The values obtained for the tested systems are in Table 2. As expected, the highest values of volumetric mass transfer coefficients were obtained for ammonia solutions containing 1,4-butanediol and 1,6-hexanediol, and the lowest values for ammonia solutions with 1,5-pentanediol. The addition of SiO_2 particles did not significantly affect this coefficient. The obtained K_Ga values in the tested ammonia solutions of concentration 1.5 mol/dm^3 are higher than those determined in a similar system but in ammonia solutions with a lower concentration (0.53 mol/dm^3) [27]. This is consistent with the research results presented by other researchers, as an increase in NH_3 concentration increases the absorption rate and higher values of volumetric mass transfer coefficients [16,38,39].

Based on the obtained results of CO_2 absorption in ammonia solutions with tested additives, it can be concluded that the presence of EG, PRD, BUD, and HED diols significantly improves the efficiency of carbon dioxide absorption. Under the tested conditions, after 1 h, the highest amount of CO_2 was captured in the solution containing BUD, which absorbed 0.31 mol of CO_2 per mol of NH_3. However, in the ammonia solution without any additives, the loading was 0.25 mol CO_2 per mol NH_3. The addition of fine SiO_2 particles to solutions from EG, PRD, BUD, and HED slightly increased the amount of CO_2 removed from the gas stream. The best result was also obtained in the solution with BUD when the CO_2 loading was 0.32 mol CO_2 per mol NH_3. The positive impact of the increase in the carbon chain length on the CO_2 absorption rate in the tested systems for EG, PRD, BUD, and HED is due to several factors. First, these molecules reduce gas bubble size by adsorbing on the gas-liquid interface, which results in a higher surface of mass transfer. Moreover, the longer carbon chain length in the diol results in a better effect on inhibiting the escape of ammonia and will be discussed in Chapter 3.3. Solutions containing PED exhibited different behavior, as the addition of this organic compound resulted in deterioration of CO_2 capture and slower absorption. Anomalies in the properties of aqueous solutions of this diol have been previously reported, e.g., surface tension of aqueous solutions. A comparison of the relative CO_2 loading in the tested solutions after 1 h of absorption is shown in Fig. 4. The relative CO_2 loading

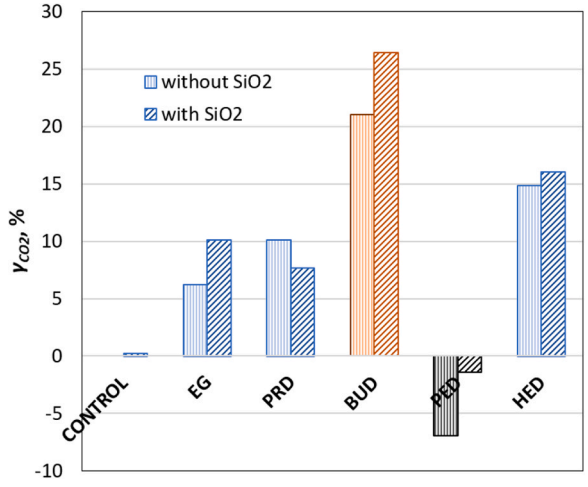

Fig. 4. Relative CO_2 loading after 1 h of carbon dioxide absorption in the tested solutions.

was calculated as:

$$\gamma_{CO2} = \frac{\Delta n_{CO2,ad} - \Delta n_{CO2,contr}}{\Delta n_{CO2,contr}} \bullet 100\% \quad (16)$$

Where $\Delta n_{CO2,ad}$ and $\Delta n_{CO2,contr}$ are the number of moles of carbon dioxide captured in the solvents with additives and pure ammonia solution, respectively.

3.3. Ammonia desorption

Changes in the concentration of ammonia in the outlet gas from the absorber over time are presented in Figs. 5 and 6. Two ranges can be distinguished on all recorded curves, characterizing the escape of ammonia. In the first stage, the maximum ammonia concentration is initially reached, then the ammonia content in the exhaust gas decreases quite quickly. In the second stage, after approximately 1000 s, the ammonia concentration in the gas decreases very slowly. The observed course of the ammonia concentration in the exhaust gas over time can be related to the pH of the solution. At the beginning of the experiment, the pH of the solution is high and is approximately 11.6. Therefore, the equilibrium of the NH_3 dissociation reaction (Eq. 14) is shifted towards the formation of free ammonia, and this intensifies its escape from the solution. As the absorption of CO_2 in the solution progresses, the pH of the solvent decreases, which causes the lowering of the free NH_3 concentration in the solution, and the concentration of ammonium ions increases. This causes the amount of desorbed ammonia to decrease significantly.

Based on the molar flux of air introduced into the absorber and the concentration of ammonia in the outlet stream at define time of experiments, the relative ammonia desorption was calculated as:

$$\beta_{NH3} = \frac{n_{out,NH3}}{n_{in,NH3}} \bullet 100\% \quad (17)$$

where: β_{NH3} is the relative ammonia desorption, $n_{out,NH3}$ is the number of moles of ammonia desorbed during gas flow, and $n_{in,NH3}$ is the number of moles of ammonia introducing to the reactor with the define volume of solvent. The obtained β_{NH3} values are collected in Table 3.

Based on these results, it can be concluded that the highest desorption of NH_3 from solvents was in pure ammonia solution. BUD and HED showed only slight slowdowns in ammonia escape, and PED had the best properties in inhibiting this phenomenon. However, a significant improvement in retaining ammonia in the absorbent was when silica was added to the solvents. During CO_2 absorption in all tested solvents with SiO_2, the escape of ammonia was lower than in solutions without the addition of solids. The highest reduction in desorption was achieved for a pure ammonia solution, and the absolute least amount of NH_3 escaped when PED was in the solution.

The ammonia molar flux was calculated as follows:

$$Q_{NH3} = \left(Y_{out,NH3} - Y_{in,NH3}\right) Q_{air} \quad (18)$$

where Q_{NH3} is the molar flux of ammonia, Q_{air} is the molar flux of air, $Y_{out,NH3}$ and $Y_{in,NH3}$ are relative molar fractions of ammonia in the outlet and inlet gas streams, respectively.

During gas flow through the NH_3 solution, ammonia desorption occurs from the liquid phase to the gas phase. The mass transport rate can be calculated using the equation:

$$N_{NH3} = K_L\left(C_{L,NH3} - C_{G,NH3}\right) \quad (19)$$

where K_L is the overall mass transfer coefficient in a liquid phase, $C_{L,NH3}$ is the concentration of free ammonia in the solution and $C_{G,NH3}$ is the equilibrium concentration of ammonia with the respect to its content in the gas phase. The concentration of free ammonia in the solution was calculated based on the dissociation constant of ammonia and the pH value. The equilibrium concentration was determined from Henry's law,

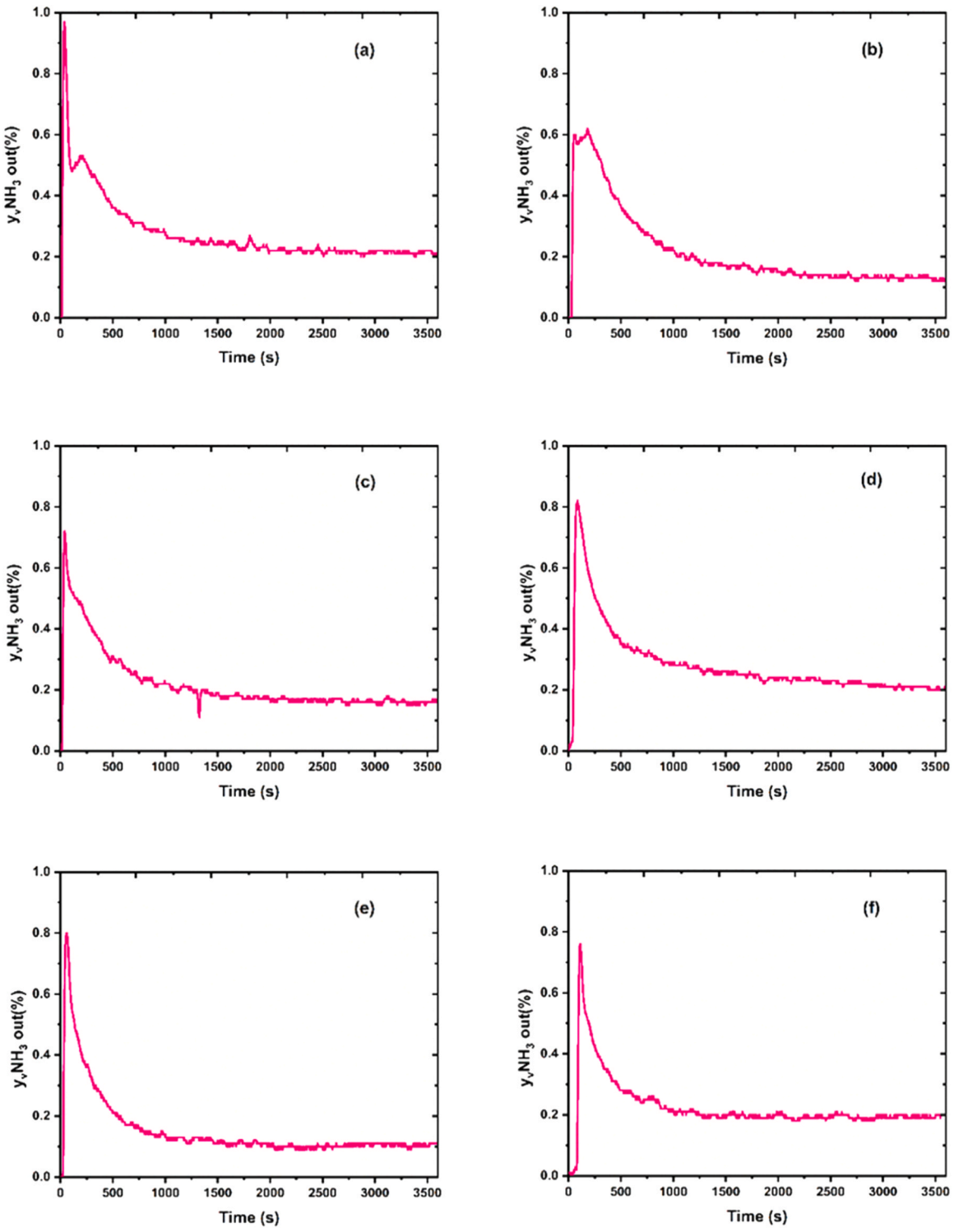

Fig. 5. NH_3 concentration (in mole fraction) in the gas flowing out during CO_2 absorption in ammonia solution: (a) without additives; (b) with EG; (c) with PRD; (d) with BUD; (e) with PED; (f) with HED.

in which the partial pressure of ammonia was the arithmetic mean of the NH_3 concentration in the gas stream at the inlet and outlet of the absorber [16]:

$$C_{G,NH3} = \frac{\left(y_{in,NH3} + y_{in,NH3}\right)}{2} \frac{P}{H_w^{NH3}} \tag{20}$$

where $y_{in,NH3}$ and $y_{in,NH3}$ are the mole fraction of ammonia in the inlet and outlet gas streams, P is the total pressure, and H_w^{NH3} is the Henry's constant determined from the equation [37]:

$$H_w^{NH3} = \frac{1}{0.59} \exp\left[-4200\left(\frac{1}{T} - \frac{1}{298.15}\right)\right] \tag{21}$$

The molar flow rate of ammonia during the desorption from the liquid to the gas phase can be calculated as:

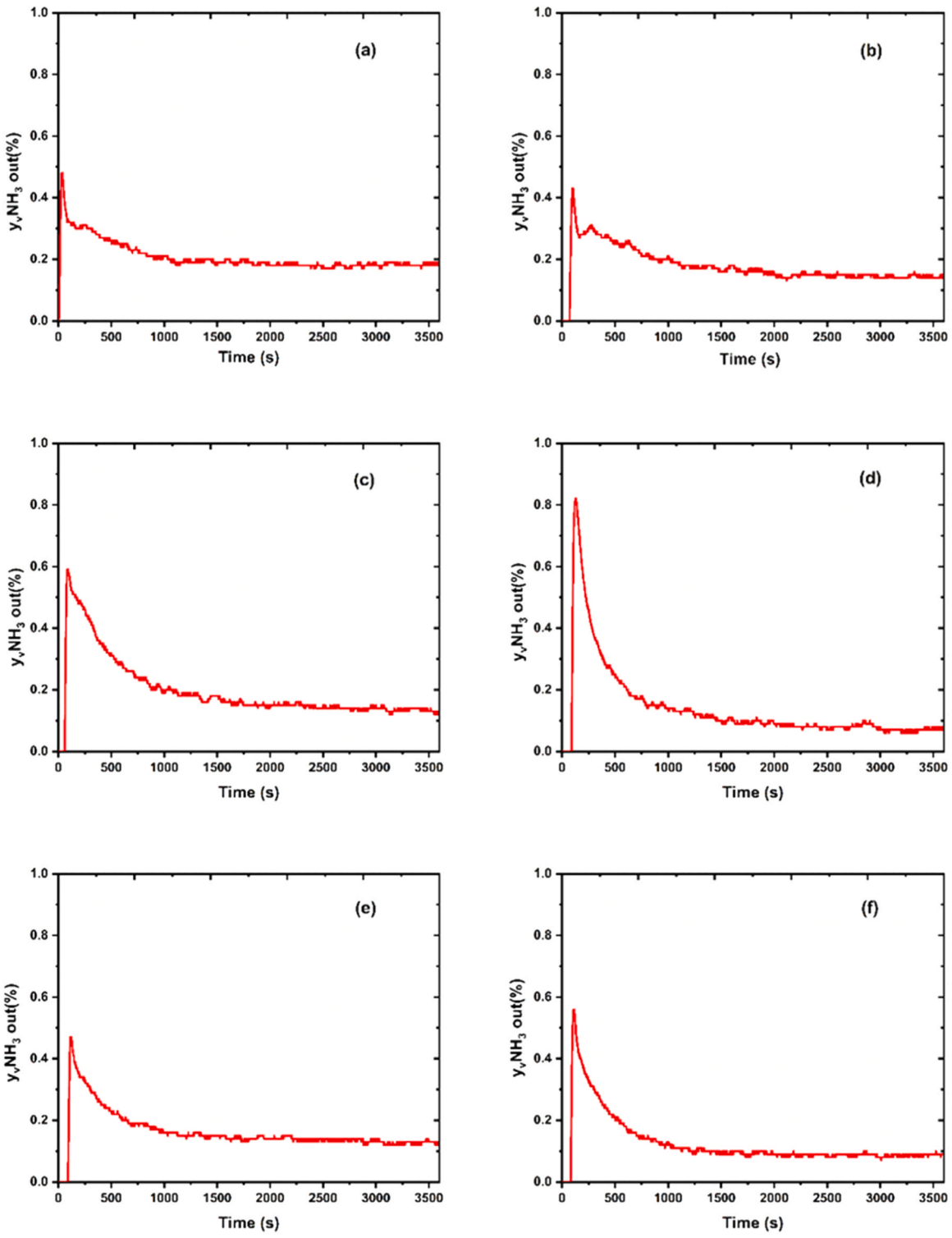

Fig. 6. NH_3 concentration (in mole fraction) in the gas flowing out during CO_2 absorption in ammonia solution containing 0.05 wt% colloidal SiO_2: (a) without diols; (b) with EG; (c) with PRD; (d) with BUD; (e) with PED; (f) with HED.

$$N_{NH3} = \frac{Q_{NH3}}{A} = \frac{\left(Y_{out,NH3} - Y_{in,NH3}\right)Q_{air}}{aV_L} \tag{22}$$

Using Eqs. (18) – (22), the volumetric mass transfer coefficients K_La were calculated for the tested systems, and the values are presented in Table 3.

A comparison of the effectiveness of ammonia retention in the presence of the tested diols and SiO_2 is shown in Fig. 7. The relative NH_3 desorption inhibition of the additives used was determined as:

$$\gamma_{NH3} = \frac{n_{NH3,contr} - n_{NH3,add}}{\Delta n_{NH3,contr}} \bullet 100\% \tag{23}$$

where $n_{NH3,contr}$ is the number of moles of ammonia that escaped from the control solution (without additives), and $n_{NH3,add}$ is the number of moles of ammonia desorbed from the solution containing additives.

Analyzing the data presented in the graph, it can be concluded that

Table 3
Relative ammonia desorption (β_{NH3}) and overall volumetric mass transfer coefficient of NH_3 desorption (K_La) in ammonia solutions with the tested additives.

Solution	β_{NH3}, %		$K_La \cdot 10^5$, mol·m^{-3}·s^{-1}·Pa^{-1}	
	without SiO_2	with SiO_2	without SiO_2	with SiO_2
Control	0.62	0.45	2.80	1.64
EG	0.58	0.51	2.24	1.98
PRD	0.57	0.54	2.34	1.78
BUD	0.60	0.53	2.87	1.73
PED	0.46	0.40	2.00	1.85
HED	0.62	0.54	2.56	1.86

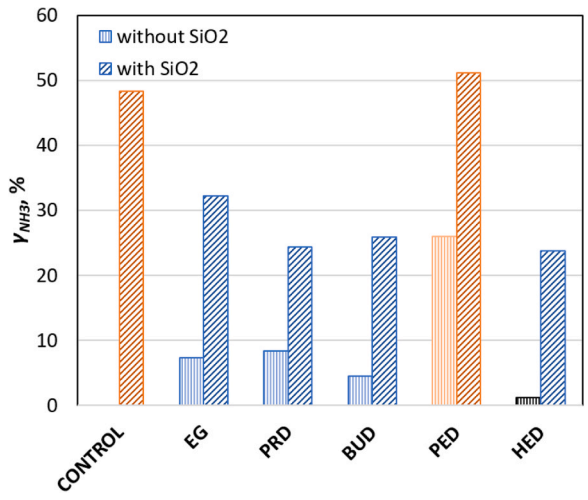

Fig. 7. Relative inhibition of ammonia desorption with tested additives.

PED had the best inhibitory effect among the diols used, and HED was the least effective. In all tested systems, SiO_2 particles intensely slowed down the escape of ammonia. The silica particles inhibited the escape of NH_3 from the pure ammonia solution and the solution with the addition of PED most effectively. A correlation can be between carbon dioxide absorption and ammonia desorption in these solutions, i.e., both slower CO_2 absorption and NH_3 desorption were observed in pure ammonia solution and the PED solvent.

The influence of solid particles on the mass transfer rate is not clearly explained [40]. Most often, it is indicated that an increase in the concentration of solid particles reduces the value of the volumetric mass transfer coefficient. However, an increase in the mass transport rate was observed for low solid concentrations (up to 5% vol.) [41,42]. This is because solid particles in the liquid phase can cause opposing effects. Firstly, they affect the viscosity of the suspension. Furthermore, in non-uniform flows, increasing the concentration of solid particles may intensify the coalescence of bubbles, which leads to a reduction of the gas-liquid interface. On the other hand, when some of the particles move to the surface of the gas bubbles, it leads to the formation of local turbulence and an increase in the mass transfer coefficient on the liquid side [40,43]. Moreover, in the case of a solution containing ammonia, its adsorption on the silica surface [44] may slow down its desorption from the liquid to the gas phase.

4. Conclusions

Ammonia solutions as an absorbent for carbon dioxide capture have many advantages over the most commonly used MEA solutions. First of all, ammonia is not easily degraded, requires less energy than processes involving amines, and the equipment does not rust. However, one of the most serious disadvantages of this solvent is its high volatility, which causes ammonia to escape when the gas flows through the absorbent. Therefore, this research focused on searching for a way to reduce the degree of ammonia escape by adding selected α,ω-diols and the addition of fine silica particles. Two series of solvents based on ammonia solutions were tested: i) with ethylene glycol (EG), 1,3-propanediol (PRD), 1,4-butanediol (BUD), 1,5-pentanediol (PED), and 1,6-hexanediol (HED) and ii) solutions containing, in addition to diols, SiO_2 particles. The studies showed that CO_2 absorption occurred faster in ammonia solutions with EG, PRD, BUD, and HED, and the CO_2 loading was higher than in pure NH_3 solution. However, solutions with PED were characterized by a lower CO_2 absorption rate and a lower CO_2 loading after a fixed time. The most effective additive improving CO_2 absorption was BUD, followed by HED. SiO_2 particles improved slightly the absorption efficiency in most of the tested diol solutions.

All diols used inhibited the escape of ammonia, with PED having the most effective effect. However, adding silica particles was a very effective inhibitor of ammonia escape. The presence of colloidal SiO_2 slowed the escape in all systems tested, and the reduction was over 20% compared to the pure ammonia solution. The highest impact was measured in the NH_3 solution with PED and without additives, i.e., 51% and 48% relative reduction in NH_3 desorption, respectively.

Taking into account the effect of the additives used on the absorption of CO_2 and the effectiveness of inhibiting the escape of NH_3 from the solution, the best combination tested is the use of BUD and SiO_2. The addition of this diol and colloidal SiO_2 resulted in an increase in CO_2 loading by 26% and reduced ammonia desorption by 26%.

CRediT authorship contribution statement

Amibo Temesgen Abeto: Data curation, Investigation, Methodology, Writing – original draft. **Konopacka-Lyskawa Donata:** Conceptualization, Data curation, Formal analysis, Funding acquisition, Supervision, Validation, Visualization, Writing – original draft, Writing – review & editing.

Declaration of Competing Interest

The authors declare that they have no known competing financial interests or personal relationships that could have appeared to influence the work reported in this paper.

Data availability

Data will be made available on request.

Acknowledgements

This work was supported by Faculty of Chemistry, Gdańsk University of Technology [grant number 036934].

References

[1] R. Sellevold, M. Vizcaíno, Global warming threshold and mechanisms for accelerated greenland ice sheet surface mass loss, J. Adv. Model. Earth Syst. 12 (2020), https://doi.org/10.1029/2019MS002029.
[2] C.P. Leisner, Review: climate change impacts on food security- focus on perennial cropping systems and nutritional value, Plant Sci. 293 (2020) 110412, https://doi.org/10.1016/j.plantsci.2020.110412.
[3] M.M. Ramirez-Corredores, M.R. Goldwasser, E. Falabella de Sousa Aguiar, Carbon Dioxide and Climate Change, in: 2023: pp. 1–14. https://doi.org/10.1007/978–3-031–19999-8_1.
[4] A. Tarafdar, G. Sowmya, K. Yogeshwari, G. Rattu, T. Negi, M.K. Awasthi, A. Hoang, R. Sindhu, R. Sirohi, Environmental pollution mitigation through utilization of carbon dioxide by microalgae, Environ. Pollut. 328 (2023) 121623, https://doi.org/10.1016/j.envpol.2023.121623.
[5] USGCRP Indicator Details | GlobalChange.gov, (n.d.). https://www.globalchange.gov/browse/indicators/atmospheric-carbon-dioxide ((accessed September 23, 2023).
[6] A. Raihan, A. Tuspekova, Toward a sustainable environment: nexus between economic growth, renewable energy use, forested area, and carbon emissions in

Malaysia, Resour. Conserv. Recycl. Adv. 15 (2022) 200096, https://doi.org/10.1016/j.rcradv.2022.200096.
[7] R.M. Cuéllar-Franca, A. Azapagic, Carbon capture, storage and utilisation technologies: a critical analysis and comparison of their life cycle environmental impacts, J. CO_2 Util. 9 (2015), https://doi.org/10.1016/j.jcou.2014.12.001.
[8] S. Mirzaei, A. Shamiri, M.K. Aroua, A review of different solvents, mass transfer, and hydrodynamics for postcombustion CO_2 capture, Rev. Chem. Eng. 31 (2015), https://doi.org/10.1515/revce-2014-0045.
[9] M. Bui, C.S. Adjiman, A. Bardow, E.J. Anthony, A. Boston, S. Brown, P.S. Fennell, S. Fuss, A. Galindo, L.A. Hackett, J.P. Hallett, H.J. Herzog, G. Jackson, J. Kemper, S. Krevor, G.C. Maitland, M. Matuszewski, I.S. Metcalfe, C. Petit, G. Puxty, J. Reimer, D.M. Reiner, E.S. Rubin, S.A. Scott, N. Shah, B. Smit, J.P.M. Trusler, P. Webley, J. Wilcox, N. Mac Dowell, Carbon capture and storage (CCS): the way forward, Energy Environ. Sci. 11 (2018) 1062–1176, https://doi.org/10.1039/C7EE02342A.
[10] A. Dibenedetto, A. Angelini, P. Stufano, Use of carbon dioxide as feedstock for chemicals and fuels: homogeneous and heterogeneous catalysis, J. Chem. Technol. Biotechnol. 89 (2014) 334–353, https://doi.org/10.1002/jctb.4229.
[11] E. Alper, O. Yuksel Orhan, CO_2 utilization: developments in conversion processes, Petroleum 3 (2017) 109–126, https://doi.org/10.1016/j.petlm.2016.11.003.
[12] N. Czaplicka, D. Konopacka-Łyskawa, Utilization of gaseous carbon dioxide and industrial Ca-Rich waste for calcium carbonate precipitation: a review, Energies 13 (2020), https://doi.org/10.3390/en13236239.
[13] B. Bouargane, M.G. Biyoune, A. Mabrouk, A. Bachar, B. Bakiz, H. Ait Ahsaine, S. Mançour Billah, A. Atbir, Experimental investigation of the effects of synthesis parameters on the precipitation of calcium carbonate and portlandite from moroccan phosphogypsum and pure gypsum using carbonation route, Waste Biomass Valoriz. 11 (2020), https://doi.org/10.1007/s12649-019-00923-3.
[14] F. Wang, J. Zhao, H. Miao, J. Zhao, H. Zhang, J. Yuan, J. Yan, Current status and challenges of the ammonia escape inhibition technologies in ammonia-based CO_2 capture process, Appl. Energy 230 (2018), https://doi.org/10.1016/j.apenergy.2018.08.116.
[15] S. Ma, G. Chen, R. Gao, J. Wen, L. Ma, Experimental research of ammonia escape in CO 2 absorption using ammonia solution in wetted-wall column, Int. J. Greenh. Gas. Control. 51 (2016) 254–259, https://doi.org/10.1016/j.ijggc.2016.05.022.
[16] S. Ma, G. Chen, S. Zhu, T. Han, W. Yu, Mass transfer of ammonia escape and CO_2 absorption in CO_2 capture using ammonia solution in bubbling reactor, Appl. Energy 162 (2016) 354–362, https://doi.org/10.1016/j.apenergy.2015.10.089.
[17] Z. Lv, K. Qiao, F. Chu, L. Yang, X. Du, Experimental study of divalent metal ion effects on ammonia escape and carbon dioxide desorption in regeneration process of ammonia decarbonization, Chem. Eng. J. 435 (2022) 134841, https://doi.org/10.1016/j.cej.2022.134841.
[18] Z. Lv, T. Wang, K. Qiao, L. Yang, X. Du, Experimental study on carbon dioxide absorption by aqueous ammonia with nickel and chromium ions in bubbling tower at low temperatures, Chem. Eng. Res. Des. 179 (2022) 298–307, https://doi.org/10.1016/j.cherd.2022.01.035.
[19] N. Czaplicka, D. Konopacka-Łyskawa, B. Kościelska, M. Łapiński, Effect of selected ammonia escape inhibitors on carbon dioxide capture and utilization via calcium carbonate precipitation, J. CO_2 Util. 42 (2020), https://doi.org/10.1016/j.jcou.2020.101298.
[20] N. Czaplicka, D. Dobrzyniewski, S. Dudziak, C. Jiang, D. Konopacka-Łyskawa, Improvement of CO_2 absorption and inhibition of NH3 escape during CaCO3 precipitation in the presence of selected alcohols and polyols, J. CO_2 Util. 62 (2022) 102085, https://doi.org/10.1016/j.jcou.2022.102085.
[21] J.-B. Seo, S.-B. Jeon, J.-Y. Kim, G.-W. Lee, J.-H. Jung, K.-J. Oh, Vaporization reduction characteristics of aqueous ammonia solutions by the addition of ethylene glycol, glycerol and glycine to the CO_2 absorption process, J. Environ. Sci. 24 (2012) 494–498, https://doi.org/10.1016/S1001-0742(11)60797-3.
[22] W. Zhang, X. Jin, W. Tu, Q. Ma, M. Mao, C. Cui, Development of MEA-based CO 2 phase change absorbent, Appl. Energy 195 (2017) 316–323, https://doi.org/10.1016/j.apenergy.2017.03.050.
[23] W. Kong, B. Lv, G. Jing, Z. Zhou, How to enhance the regenerability of biphasic absorbents for CO_2 capture: an efficient strategy by organic alcohols activator, Chem. Eng. J. 429 (2022) 132264, https://doi.org/10.1016/j.cej.2021.132264.
[24] Z. Chen, B. Yuan, G. Zhan, Y. Li, J. Li, J. Chen, Y. Peng, L. Wang, C. You, J. Li, Energy-efficient biphasic solvents for industrial carbon capture: role of physical solvents on CO_2 absorption and phase splitting, Environ. Sci. Technol. 56 (2022) 13305–13313, https://doi.org/10.1021/acs.est.2c05687.
[25] A. Tavakoli, K. Rahimi, F. Saghandali, J. Scott, E. Lovell, Nanofluid preparation, stability and performance for CO_2 absorption and desorption enhancement: a review, J. Environ. Manag. 313 (2022) 114955, https://doi.org/10.1016/j.jenvman.2022.114955.
[26] Q. Zhang, C. Cheng, T. Wu, G. Xu, W. Liu, The effect of Fe3O4 nanoparticles on the mass transfer of CO_2 absorption into aqueous ammonia solutions, Chem. Eng. Process. - Process. Intensif. 154 (2020) 108002, https://doi.org/10.1016/j.cep.2020.108002.
[27] D. Konopacka-Łyskawa, T. Amibo, D. Dobrzyniewski, M. Łapiński, Improving carbon dioxide absorption in aqueous ammonia solutions by fine SiO2 particles, Chem. Process Eng. New Front. 44 (2023).
[28] M. Deleu, M. Paquot, C. Blecker, Micellar Systems: Surface Tension Measurements, in: P. Somasundaran (Ed.), Encycl. Surf. Colloid Sci., 2nd ed., Taylor&Francis, 2006: pp. 3773–3781.
[29] K. Nakanishi, T. Matsumoto, M. Hayatsu, Surface tension of aqueous solutions of some glycols, J. Chem. Eng. Data. 16 (1971) 44–45.
[30] C.M. Romero, M.S. Páez, J.A. Miranda, D.J. Hernández, L.E. Oviedo, Effect of temperature on the surface tension of diluted aqueous solutions of 1,2-hexanediol, 1,5-hexanediol, 1,6-hexanediol and 2,5-hexanediol, Fluid Phase Equilib. 258 (2007) 67–72, https://doi.org/10.1016/j.fluid.2007.05.029.
[31] J. Gliński, G. Chavepeyer, J.-K. Platten, Untypical surface properties of aqueous solutions of 1,5-pentanediol, Colloids Surf. A Physicochem. Eng. Asp. 162 (2000) 233–238, https://doi.org/10.1016/S0927-7757(99)00207-1.
[32] P. Painmanakul, K. Loubière, G. Hébrard, M. Mietton-Peuchot, M. Roustan, Effect of surfactants on liquid-side mass transfer coefficients, Chem. Eng. Sci. 60 (2005) 6480–6491, https://doi.org/10.1016/j.ces.2005.04.053.
[33] P. Pichetwanit, S. Kungsanant, T. Supap, Effects of surfactant type and structure on properties of amines for carbon dioxide capture, Colloids Surf. A Physicochem. Eng. Asp. 622 (2021) 126602, https://doi.org/10.1016/j.colsurfa.2021.126602.
[34] G. Vázquez, G. Antorrena, J.M. Navaza, Influence of surfactant concentration and chain length on the absorption of CO_2 by aqueous surfactant solutions in the presence and absence of induced marangoni effect, Ind. Eng. Chem. Res. 39 (2000) 1088–1094, https://doi.org/10.1021/ie990644j.
[35] F. Atzori, F. Barzagli, A. Varone, G. Cao, A. Concas, CO_2 absorption in aqueous NH3 solutions: novel dynamic modeling of experimental outcomes, Chem. Eng. J. 451 (2023) 138999, https://doi.org/10.1016/j.cej.2022.138999.
[36] J.-B. Seo, S.-B. Jeon, S.-S. Lee, J.-Y. Kim, K.-J. Oh, The physical solubilities and diffusivities of N2O and CO_2 in aqueous ammonia solutions on the additions of AMP, glycerol and ethylene glycol, Korean J. Chem. Eng. 28 (2011) 1698–1705, https://doi.org/10.1007/s11814-011-0030-8.
[37] R. Sander, Compilation of Henry's law constants (version 4.0) for water as solvent, Atmos. Chem. Phys. 15 (2015) 4399–4981, https://doi.org/10.5194/acp-15-4399-2015.
[38] S. Ma, B. Zang, H. Song, G. Chen, J. Yang, Research on mass transfer of CO_2 absorption using ammonia solution in spray tower, Int. J. Heat. Mass Transf. 67 (2013) 696–703, https://doi.org/10.1016/j.ijheatmasstransfer.2013.08.090.
[39] W. Li, X. Zhao, B. Liu, Z. Tang, Mass transfer coefficients for CO $_2$ absorption into aqueous ammonia using structured packing, Ind. Eng. Chem. Res. 53 (2014) 6185–6196, https://doi.org/10.1021/ie403097h.
[40] S. Mahmoudi, M.W. Hlawitschka, Effect of solid particles on the slurry bubble columns behavior – a review, ChemBioEng Rev. 9 (2022) 63–92, https://doi.org/10.1002/cben.202100032.
[41] P. Mena, A. Ferreira, J.A. Teixeira, F. Rocha, Effect of some solid properties on gas–liquid mass transfer in a bubble column, Chem. Eng. Process. Process. Intensif. 50 (2011) 181–188, https://doi.org/10.1016/j.cep.2010.12.013.
[42] O. Ozkan, A. Calimli, R. Berber, H. Oguz, Effect of inert solid particles at low concentrations on gas–liquid mass transfer in mechanically agitated reactors, Chem. Eng. Sci. 55 (2000) 2737–2740, https://doi.org/10.1016/S0009-2509(99)00532-1.
[43] E.M. Lakhdissi, A. Fallahi, C. Guy, J. Chaouki, Effect of solid particles on the volumetric gas liquid mass transfer coefficient in slurry bubble column reactors, Chem. Eng. Sci. 227 (2020) 115912, https://doi.org/10.1016/j.ces.2020.115912.
[44] F.E. Bartell, Y. Fu, Adsorption from aqueous solutions by silica, J. Phys. Chem. 33 (1929) 676–687, https://doi.org/10.1021/j150299a004.